




Article

Effectiveness of Nature-Based Solutions in Mitigating Flood Hazard in a Mediterranean Peri-Urban Catchment

Carla S. S. Ferreira ^{1,2,3,*} , Sandra Mourato ^{4,5} , Milica Kasanin-Grubin ⁶ ,
António J. D. Ferreira ¹ , Georgia Destouni ^{2,3}  and Zahra Kalantari ^{2,3} 

- ¹ Research Centre for Natural Resources, Environment and Society (CERNAS), Polytechnic Institute of Coimbra, Coimbra Agrarian Technical School, 3045-601 Coimbra, Portugal; aferreira@esac.pt
 - ² Department of Physical Geography, Stockholm University, and Bolin Centre for Climate Research, Stockholm SE-10691, Sweden; georgia.destouni@natgeo.su.se (G.D.); zahra.kalantari@natgeo.su.se (Z.K.)
 - ³ Navarino Environmental Observatory, 24001 Messinia, Greece
 - ⁴ Polytechnic Institute of Leiria, School of Technology and Management, P.O. Box 4163, 2411-901 Leiria, Portugal; sandra.mourato@ipleiria.pt
 - ⁵ Mediterranean Institute for Agriculture, Environment and Development (MED), Universidade de Évora, Pólo da Mitra, Ap. 94, 7006-554 Évora, Portugal
 - ⁶ Institute of Chemistry, Technology and Metallurgy, University of Belgrade, 11000 Belgrade, Serbia; mkasaninrubin@chem.bg.ac.rs
- * Correspondence: carla.ssf@gmail.com

Received: 9 September 2020; Accepted: 14 October 2020; Published: 16 October 2020



Abstract: Urbanization alters natural hydrological processes and enhances runoff, which affects flood hazard. Interest in nature-based solutions (NBS) for sustainable mitigation and adaptation to urban floods is growing, but the magnitudes of NBS effects are still poorly investigated. This study explores the potential of NBS for flood hazard mitigation in a small peri-urban catchment in central Portugal, prone to flash floods driven by urbanization and short but intense rainfall events typical of the Mediterranean region. Flood extent and flood depth are assessed by manually coupling the hydrologic HEC-HMS and hydraulic HEC-RAS models. The coupled model was run for single rainfall events with recurrence periods of 10-, 20-, 50-, and 100-years, considering four simulation scenarios: current conditions (without NBS), and with an upslope NBS, a downslope NBS, and a combination of both. The model-simulation approach provides good estimates of flood magnitude (NSE = 0.91, RMSE = 0.08, MAE = 0.07, $R^2 = 0.93$), and shows that diverting streamflow into abandoned fields has positive impacts in mitigating downslope flood hazard. The implementation of an upslope NBS can decrease the water depth at the catchment outlet by 0.02 m, whereas a downslope NBS can reduce it from 0.10 m to 0.23 m for increasing return periods. Combined upslope and downslope NBS have a marginal additional impact in reducing water depth, ranging from 0.11 m to 0.24 m for 10- and 100-year floods. Decreases in water depth provided by NBS are useful in flood mitigation and adaptation within the peri-urban catchment. A network of NBS, rather than small isolated strategies, needs to be created for efficient flood-risk management at a larger scale.

Keywords: flood hazard; nature-based solutions; HEC HMS model; HEC RAS model; peri-urban catchment; mediterranean

1. Introduction

The growing global population is increasingly living in cities and this trend is expected to continue, with projections indicating that more than 60% of people globally will be living in urban areas by

2030 [1]. Peri-urban areas, i.e., rural landscapes around cities, are expected to host a significant portion of this growth [2,3]. Urban sprawl will increase social and environmental problems, since many urban settlements lie along rivers, coastlines, or both [4]. Therefore, one of the major concerns in the future will be urban water sustainability and management, in order to protect human well-being [5]. Nowadays, urban floods affect a large number of people worldwide, causing human fatalities and significant damages [6].

Urbanization considerably influences hydrological processes, by lowering infiltration, increasing runoff and triggering higher and more rapidly occurring peak streamflows [7,8], and higher recurrence of floods [4,9,10]. However, the magnitude of the hydrological changes is affected by several biophysical parameters, such as soil type, topography, the percentage of sealing and the spatial heterogeneity of the urban features [11,12]. These parameters influence the heterogeneity of rainfall-runoff dynamics and the connectivity of water fluxes within catchments [11]. Intensive rainfalls lead to high and quick runoff generation, and comprise a major cause of urban floods, together with failure of storm drainage systems [13].

Riverine floods are difficult to control, so a strategy of “living with floods” is considered more reasonable [14]. Depending on the level of risk, political decisions and funding, a suitable combination of measures should be adopted to mitigate rising flood risk driven by urbanization, but also climate change [15]. Conventional engineering solutions alone are often not enough for flood control, so nature-based solutions (NBS) are increasingly being applied in flood management [16,17]. By using flexible and cost-effective solutions which mimic natural processes, NBS has the potential to build urban resilience and provide a number of ecosystem services associated with environmental, social and economic benefits [18].

Distinct NBS strategies have been used to increase water infiltration, surface water retention and evapotranspiration, breaking flow connectivity over the landscape and thus mitigating flood hazard [19]. Application of NBS ranges from micro-scale techniques (e.g., green roofs and detention basins), implemented near runoff sources, to large-scale areas which are allowed to be temporarily flooded [20,21]. NBS based on enhancing the retention capacity in river floodplain is also widely used, and attained by changing land-use practices, afforestation or wetland restoration [22]. Although several studies address the usefulness and potential of NBS in water management, very limited information regarding their effectiveness on flood mitigation is available [23]. Furthermore, the performance of different NBS in flood protection is strongly influenced by specific local conditions, including soil type and NBS design, which bring additional challenges to understand the impact of specific NBS strategies [24].

Application of NBS demands comprehensive knowledge and evaluation, and a “one size fits all” approach cannot be applied [25]. So far, research has mostly focused on technical aspects of NBS and evaluation of a few benefits [26], while the link between NBS and the wider water system and comprehensive methodology remain to be determined [27]. Despite strong evidence that NBS are a sustainable solution for reducing urban flooding, their full effect potential is still largely unexploited [28]. The need for quantitative assessments of the effectiveness of NBS on flood mitigation have been stressed by several authors, particularly for the Mediterranean region given the limited number of studies available [16,22].

The aim of this study is to quantitatively investigate the potential of NBS to mitigate flood hazard in a small Mediterranean peri-urban catchment, under great urbanization pressure and where recurrent floods have led to property damages. The study uses hydrological and hydraulic model simulations to assess flood inundation under distinct return periods (10, 20, 50 and 100 years) for current conditions (without NBS) and three NBS scenarios: installing one NBS upslope; installing one NBS downslope; and installing a combination of upslope and downslope NBS. The NBS considered in these scenarios consist in natural inundation of abandoned areas adjacent to the stream, through a system to divert stream water during high flows.

2. Materials and Methods

2.1. Study Site

The study site is Ribeira dos Covões, a small catchment (6.2 km²) located on the outskirts of Coimbra, the largest city in central Portugal (40°13' N, 8°27' W, Figure 1a). The catchment has a south-north elongated shape, with elevation ranging from 30 to 205 m above sea level, and slopes of up to 46°, although the average slope is 9° (Figure 1b).

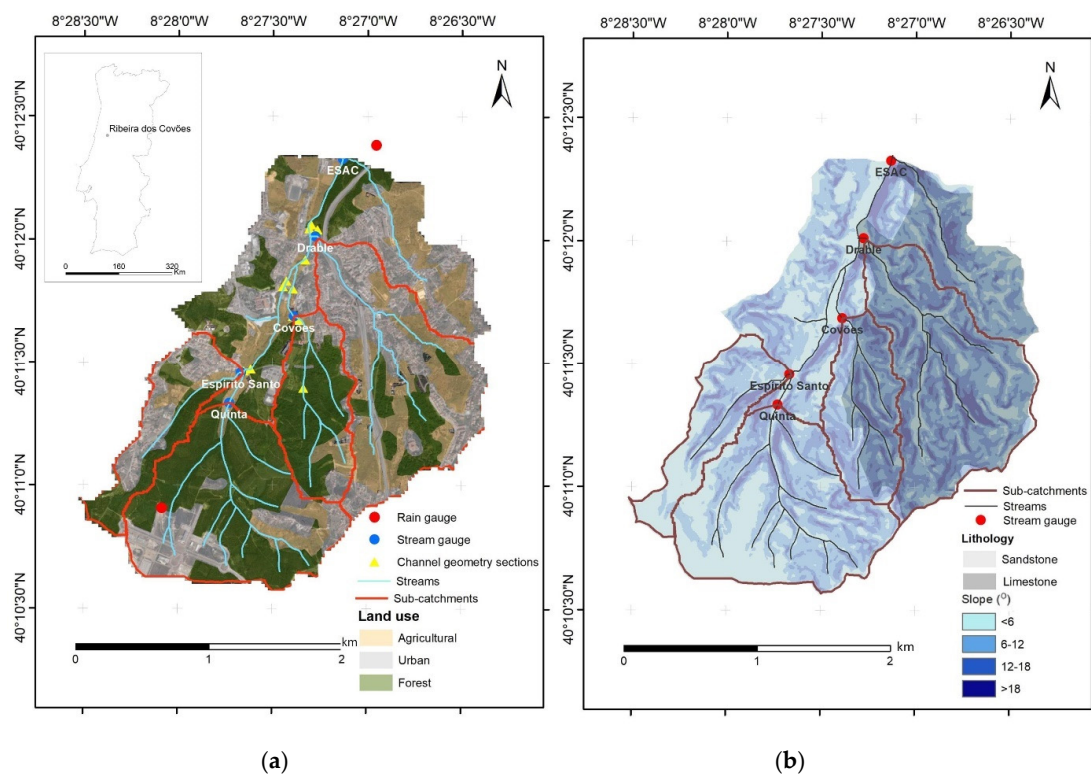


Figure 1. Location of the Ribeira dos Covões catchment in Portugal, its land use and stream network, including the hydrological monitoring network providing rainfall and streamflow data within the sub-catchment (Espírito Santo, Quinta, Covões and Drable), and of the channel cross-section profiles described during the field survey (a). (b) shows the slope and lithology within the catchment.

The catchment overlies Cretaceous and Tertiary sandstone conglomerates and mudstones in the west (56%), Jurassic dolomitic and marl-limestone units in the east (41%), and some Plio-quadernary sandy-conglomerates and alluvial deposits (3%) in the main valley. The sandstone area comprises deep (>3 m; Figure 1b) Fluvisols and Podsolis, whereas the limestone contains shallow (<0.4 m) Leptic Cambisols [29].

The climate is humid Mediterranean, with mean annual rainfall of 980 mm [30]. The catchment experiences a wetting-up period from October to February/March, and thereafter a gradual decrease in moisture conditions through spring and summer, with the latter extending from June to August and receiving only ~8% of annual rainfall [8]. This seasonal pattern causes strong variation in the hydrological regime of the catchment, which is characterized by perennial flow at the outlet, supplied by some upstream seasonal and ephemeral tributaries, and several springs located on sandstone. Baseflow represents 33–37% of annual streamflow at the catchment outlet, mainly provided by the sandstone (53%) and low-lying areas (45%), with a residual contribution from the majority of limestone extents (2%) [29]. Mean annual runoff coefficient ranges from 14% to 21%, depending on climate conditions [8].

Catchment land-use comprises 56% forest, 40% urban and 4% agricultural area (Figure 1a). The forest is dominated by *Eucalyptus globulus* L. and *Pinus pinaster* L. plantations, mostly in headwater

and western parts of the catchment, respectively, and includes a few relic oaks in the limestone areas. Agricultural land is mainly occupied by relatively small olive plantations, pasture at some sites along the main stream and domestic gardens. Urban land uses include residential areas, education and health services, and a few small shops and facilities. Urban developments are dispersed over the catchment and include contrasting urbanization patterns, ranging from older urban cores dominated by detached single-family houses surrounded by gardens, with low population density, to relatively recent apartment blocks and terrace houses characterized by continuous surface sealing and high population density. The catchment includes a business park in the southwest part, under construction over the last 10 years and covering ~5% of the catchment area. It also contains an extensive network of roads, including a motorway extending north-south along the catchment. In 2011, Ribeira dos Covões had around 26,600 inhabitants [31].

Within the urban areas, storm runoff from sealed surfaces (e.g., roads and buildings) in the low-density urban cores is partially dissipated in surrounding pervious soils, such as agricultural and woodland soils. In contrast, storm runoff from the medium- and high-density urban cores is directed via drains and pipes to the stream network. The storm runoff from the business park is piped to a detention basin, which slows down its release to the stream network. Wastewater is routed through a separate sewerage system to a treatment plant placed outside the catchment.

The Ribeira dos Covões catchment has historically suffered from flooding triggered by intense rainfall events, causing damage to agriculture and some downslope urban areas, and constraints on road traffic mostly at downslope sites. The largest flood to date was recorded in October 2006, triggered by rainfall of 102 mm/day (return period 50 years), but older residents report major floods around 1936 and 1966 [15]. In recent years, an increasing number of minors localized flood events have been recorded, triggered by (i) increasing stream discharge driven by urbanization, particularly after construction of the business park according to residents and previous studies [8,15,29]; and (ii) a reduction in the drainage capacity of hydraulic infrastructure (e.g., drains and pipes), caused by siltation driven by soil erosion, mostly from construction sites [32], and by lack of maintenance. Floods are mostly observed at the end of the dry summer season, when short but very intense rainfall events occur, as is typical in the Mediterranean region [33].

2.2. Hydrologic and Hydraulic Modelling

2.2.1. Modelling Overview

The simulations in this study is performed using the physically-based semi-distributed Hydrologic Engineering Center (HEC) model (open-source software), by coupling the model packages “Hydrologic Modelling System” (HMS) and “River Analysis System” (RAS). The hydrologic HEC-HMS and hydraulic HEC-RAS modelling tools have been used in numerous past studies to investigate runoff and floodplain inundation in various geographical areas, including large river basins and small urban or natural catchments [12,34,35]. HEC-RAS is one of the most known, analyzed and used models for flood mapping both in the scientific literature and in practice [36]. Given the wide application and reliability of HEC model it was considered appropriate to develop the current study.

HEC-HMS is a hydrologic model designed to simulate precipitation-runoff processes in catchment systems [37]. The catchment system is separated in elements of the system (sub-catchments), performing different functions of the rainfall-runoff process, thus, representing for example a surface runoff or a stream channel. HEC-HMS computes distributed runoff by using grid-cell depiction of the catchment. It is based on a water balance equation and uses a variety of mathematical models for simulating precipitation, evapotranspiration, infiltration, surface runoff, baseflow and open channel routing. The model categorizes all land types and water in a catchment as either (i) directly connected impervious surface, contributing to precipitation runoff without volume losses; or (ii) pervious surface, where precipitation is subject to losses [38,39].

The physical process in each system is represented by mathematical relations defined for particular attributes of the system. These relations can be empirically derived or defined from a few parameters based on field observations and measurements. The model output is the computation of streamflow hydrographs [40].

HEC-HMS is one of the few hydrologic models to include both event and continuous simulation capabilities. This flexibility allows the model to be used for different purposes with minimum effort (e.g., a model developed to assess floods can be repurposed to investigate water supply) [41]. Details about the model structure, the processes involved and the applications of the model are provided in the User's Manual [38] of HEC-HMS.

The HEC-RAS tool simulates runoff hydraulics through the channel (based on channel morphology) and can generate the extent of the inundated area, the water depth and flow velocity. It is designed to perform 1D and 2D hydraulic calculations for a full network of natural and constructed channels, floodplains, etc. [38]. HEC-RAS includes (i) a steady-state surface flow simulation, to calculate water surface profiles for steady gradually varied flow; and (ii) an unsteady surface flow simulation, capable of simulating 1D, 2D and a combination of 1D and 2D unsteady flows, through a full network of open channels, floodplains and alluvial fans [36]. HEC-RAS has been used in a wide range of hydraulic studies to characterize the flood hazard in space and time (e.g., water depth, flow rate, flow velocity), giving greater realism and accuracy of results [36,41–43]. A full description of the model and its computational schemes can be found in USACE [28].

2.2.2. Input Data

The HEC models require several hydrological and cartographic input datasets. In the present study, these were taken from previous studies in the Ribeira dos Covões catchment, based on field data measurements. The hydrological data consists of rainfall, streamflow records (including discharge data and gauge heights) and discharge hydrographs obtained from the automatic hydrological network installed in the study catchment, which comprises two rain gauges and five streamflow gauges (Figure 1a) [29]. The hydrological data, with resolution of 5-minute intervals, is available for a three-year period, from October 2010 to September 2013. Weighted average rainfall, based on Thiessen polygon, is considered, assuming that rainfall depth at any point within the catchment is the same as the rainfall depth at the nearest gauge. The average values were considered in the model, assuming a uniform rainfall distribution across the catchment, given the similarities recorded in the datasets provided by both rain gauges [15]. The rainfall input dataset includes the intensity–duration–frequency (IDF) curve established for the Coimbra region by Brandão et al. [44], for return periods of 10, 20, 50 and 100 years.

The cartographic input dataset includes delineation of the catchment and four upstream sub-catchments (Drable, Covões, Quinta and Espírito Santo, defined by the location of the gauging stations) and a digital elevation model (DEM) with grid size 5 m, all from Ferreira et al. [29]. Land use data for 2012 (scale 1:10,000) is taken from Kalantari et al. [15]. Spatial information on geological formations and soil type is taken from Ferreira et al. [45,46].

Detailed information on the stream channel bed was collected during a field survey performed in May 2018. Thirteen cross-sections were selected over the stream network (Figure 1), based on their representativeness and site accessibility. All sites were recorded using ground global positioning system (GPS) equipment, and longitudinal and perpendicular measurements were taken manually to accurately estimate the river channel.

A detailed description of the urban storm drainage system is not available and it is thus not included in the model. Although runoff is either dispersed in pervious surrounding areas and/or piped to the nearest stream channel, the lack of information about the artificial drainage system is a source of model uncertainty.

2.2.3. Model Set-Up and Parameterization

The HEC-HMS model Version 4.2.1 is used for hydrologic modelling of Ribeira dos Covões catchment, by constructing a catchment model containing a basin model, a meteorological model and control specifications. The HEC-HMS model comes with an Arc-View extension (HEC-GeoHMS), which is used for terrain pre-processing and automatic construction of the basin model in HEC-HMS. Terrain pre-processing consists in (i) filling the sinks of DEM (cells with no clear or defined drainage direction); (ii) correcting flow direction from the filled grid, based on the premise that water flows downhill, and will follow the steepest descent direction; and (iii) calculating flow accumulation (number of cells that drain into an individual cell in the grid) from the derived flow direction grid. A hydrologically corrected DEM is required to precisely depict the flow of water through the catchment [39]. Together with basin processing (using catchment and sub-catchment input data), the model delineates the drainage system. The basin model includes the files containing the hydrological elements (sub-catchments and stream reaches) and their connectivity.

The meteorological model in the HEC-HMS for Ribeira dos Covões is set up by entering 5-min rainfall data for the three hydrological years. In the current study, precipitation excess is simulated for event modeling using the Soil Conservation Service (SCS) curve number (CN) method, according to Equation (1) [38]:

$$P_e = \frac{(P - 0.2S)^2}{P + 0.8S} \quad (1)$$

where P_e is the accumulated precipitation excess at time t ; P is the accumulated rainfall depth at time t , and S is the potential maximum retention, a measure of the ability of a catchment to abstract and retain storm precipitation. Until the accumulated rainfall exceeds the initial abstraction, the precipitation excess and hence the runoff, will be zero. Incremental precipitation excess for a time interval is computed as the difference between the accumulated excess at the end and beginning of the period. The maximum retention, S , and catchments characteristics are related through an intermediate parameter, CN, based on Equation (2) [38]:

$$S = \left(\frac{25400 - 254 \text{ CN}}{\text{CN}} \right) \quad (2)$$

CN is a hydrological coefficient representing surface runoff potential, estimated for the catchment and each upstream sub-catchment as a function of land use, soil type and antecedent moisture [27]. CN was estimated based on CN tables developed by the SCS [47], based on data collected from COS2018 and the European Soil Database v2 Raster.

Excess precipitation is then transformed into surface runoff using the SCS Unit Hydrograph for each sub-catchment and catchment, based on Equation (3) [40]:

$$U_p = C \left(\frac{25400 - 254 \text{ CN}}{\text{CN}} \right) \quad (3)$$

where U_p is the unit hydrograph peak; and C is a conversion constant (2.08).

The time of peak (T_p), related to the duration of the unit of excess precipitation, was simulated according to Equation (4):

$$T_p = \frac{\Delta t}{2} + t_{lag} \quad (4)$$

where Δt is the excess precipitation duration (which is also the computational interval in the run); and t_{lag} is the basin lag, defined as the time difference between the center of rainfall excess mass and the peak of the unit hydrograph. In this study, t_{lag} , also named SCS lag, was parameterized.

The flow in open channels is simulated using the 1D Lag method, considering the outflow hydrograph of each sub-catchment as the inflow hydrograph of the Ribeira dos Covões catchment,

but with all ordinates translated (lagged in time) by a specific duration. The flows are not attenuated, so the shape is not changed. The downstream ordinates are computed through Equation (5) [40]:

$$O_t = I_t \text{ if } t < t_{\text{lag}} \text{ or } O_t = I_{t-\text{lag}} \text{ if } t \geq \text{lag} \quad (5)$$

where O_t is the outflow hydrograph ordinate at time t ; I_t is the inflow hydrograph ordinate at time t , and lag is the time by which the inflow ordinates are to be lagged.

The unit hydrograph is used since it is one of the best methods for deriving discharge for various return periods when only 1–3 years of records are available, and when estimates of the probable maximum flood are required [48], as in the present study. The control specification containing all the timing information (start and end time of each rainfall event) for the model is built by determining time steps [37], including start and stop dates (1 October 2010 and 30 September 2013, respectively), and time of the simulation (5 min was chosen since it is the resolution of the rainfall and discharge data).

The initial conditions of the model are the calibrated values at which the HEC-HMS equation solvers begin the solution of the unsteady flow equations included in the methods. For channel methods, the initial conditions are the initial flows, and for catchment methods, the initial conditions are the initial moisture states in the catchment. The main boundary condition in HEC-HMS is precipitation, which causes runoff at sub-catchment and catchment scales. The boundary conditions to the channel reaches (routing method) are the upstream (inflow) flow hydrographs. These boundary conditions are the same for all return periods, although using different hydrographs. Parameterization of the model includes CN, as well as SCS lag and routing lag, first estimated by the basin geometric features. The model output consists of discharge hydrographs defined for each sub-catchment and catchment outlet, saved as time series data and input directly into the hydraulic model.

The HEC-RAS hydraulic model Version 5.0.5 is used. Pre-processing of the geometric input dataset is conducted in RAS Mapper, which is also used to derive triangular irregular network (TIN) data from the DEM. The TIN data are used to derive channel geometry, with manual enhancement according to cross-section profiles described during the field survey (Figure 1). The initial conditions of the model are the flow data at each reach, manually integrated through coupling with HEC-HMS model. The computations of water surface elevations are performed with the full 2D unsteady flow model in a 2D mesh, including the upstream and downstream boundary conditions. In a subsequent step, flow conditions, boundary conditions and Manning's values for each cross-section are established. Manning's n roughness coefficient, which represents resistance of a surface to flow [35], is estimated for both channel and floodplain, by combining land use data, channel bed characteristics identified during the field survey and tables of Manning's n values found in Chow [49]. Since the selected flow regime is subcritical, the boundary conditions are defined at the downstream end of the river by the normal depth, which is the slope of the river bed. Based on all this information and hydrograph outputs from the HEC-HMS model (upstream boundary conditions), the HEC-RAS model is used to solve a 2D unsteady flow equation at 5-minute resolution, using a diffusive wave approach of the Shallow water equation (Equation (6)), since it takes a shorter computational time than the full momentum alternative process. Each cell in the computational mesh makes up a control volume for which the water surface elevation and flow across the faces is to be solved [40].

$$\frac{\partial H}{\partial t} - \nabla \cdot \frac{(R(H))^{\frac{5}{3}}}{n|\nabla H|^{\frac{1}{2}}} \nabla H + q = 0 \quad (6)$$

where R is the hydraulic radius, ∇H is the surface elevation gradient, q is a source/sink flux term, ∇ is the vector of the partial derivative operators, and n is the empirically derived Manning's n .

The final model features included a 2D mesh with 35 302 cells and 5 m cell size (which is the same for all the four scenarios investigated, since the hydraulic model uses the terrain properties modified in the DEM to consider each NBS scenario), a hydrograph output interval of 5 min, and a computation

time step interval of 10 s. This time step enables a Courant number of 1.0 (or less), which is required for accuracy and stability of the model [38].

2.2.4. Model Calibration and Validation

The discharge data recorded over three hydrological years (2010/2011–2012/2013) at the five gauging stations are divided into individual storm events, defined as the period from the beginning of rainfall to the cessation of stormflow [29]. The largest and/or most intensive storm events recorded (with greatest rainfall depth and intensity during 15 min) are used for HEC model testing (calibration and validation), including both the hydrologic and hydraulic models. Given the rainfall pattern recorded during the three hydrological years, the selected storm events (Table 1) are associated with return periods of only 2 years [29]. A 5-minute time step is used for the simulation, but an hourly adjustment is performed given the small water heights and quick response time of the sub-catchments [29].

HEC-HMS is calibrated for the Ribeira dos Covões catchment outlet and the four upstream sub-catchment outlets, based on streamflow observations during five selected storm events. The automatic calibration of HEC-HMS uses the Univariate Gradient optimization algorithm, and the Peak-Weighted RMS Error objective function is minimized. The calibration is focused on the most sensitive parameters, including CN, SCS lag and routing lag, in order to produce the best fit between model results and observations, thus improving model predictability. The calibration is first performed focusing on modification of parameters at the sub-catchment scale, and then at the catchment outlet scale. The model parameters obtained are then validated using three different storm events. Optimal CN parameter values used to run the model were 61.0 in Espírito Santo, 66.7 in Quinta, 71.3 in Covões and 83.2 in Drable sub-catchments. Optimal SCS lag values ranged from 70.0 min in Espírito Santo sub-catchment to 47.7 min in Drable sub-catchment. The optimized routing lag parameter used to run the model ranged from 2.1 min to 13.8 min within the different stream sections considered. Four evaluation criteria are used to assess model performance, defined as the goodness of fit between observed and simulated streamflow: Nash–Sutcliffe efficiency (NSE) [50], root mean square error (RMSE) [51], mean absolute error (MAE) [52] and coefficient of determination (R^2) [53]. A model of sufficient quality has daily NSE between 0.5 and 0.65 [54], although lower values are acceptable for sub-daily results, since performance improves as time interval increases [55]. A model with RMSE and MAE values of zero would indicate a perfect fit to the data, whereas an optimal fit is traduced by a R^2 value of 1.

The outputs of the calibrated and validated HEC-HMS model are used as input datasets for HEC-RAS calibration and validation. HEC-RAS calibration are based on a single storm event, selected from the five events used in HEC-HMS calibration according to the best goodness-of-fit results, since the hydrologic model will run with the parameterization associated with this event. The calibration of HEC-RAS at the event-based level is conducted by changing the Manning's n value to make the simulated water depth as similar as possible to the depth measured at the catchment outlet. The calibrated model is then validated against the three storm events used in HEC-HMS validation. The optimal Manning's n value used to run the model was $0.055 \text{ s}/(\text{m}^{1/3})$. Model performance is assessed with the four evaluation criteria used for HEC-HMS. Figure 2 shows the workflow of the modeling methodology used in this study.

Table 1. Hydrological properties of the storm events used for HEC model calibration (n. 1, 4, 5, 6 and 7) and validation (n. 2, 3 and 8), including rainfall duration, depth and maximum intensity over a 15-min period (Imax), and surface runoff depth (SR) and peak discharge (PD) in the five stream gauging stations.

Storm Event n.		1		2		3		4		5		6		7		8	
Date		13/02/2011		15/02/2011		18–19/02/2011		30–31/05/2011		14/11/2011		23/09/2012		14/12/2012		08–09/03/2013	
Rainfall Duration (h)		4.6		3.2		5.4		1.3		4.7		7.8		19.6		15.9	
Rainfall (mm)		11.0		9.2		9.8		4.5		10.3		1.7		26.8		29.2	
Imax (mm/h)		11.5		19.7		5.8		6.8		15.1		4.3		3.7		18.2	
Runoff Properties		SR	PD	SR	PD	SR	PD	SR	PD	SR	PD	SR	PD	SR	PD	SR	PD
		(mm)	(L/s)	(mm)	(L/s)	(mm)	(L/s)	(mm)	(L/s)	(mm)	(L/s)	(mm)	(L/s)	(mm)	(L/s)	(mm)	(L/s)
Catchment	ESAC	0.38	707	0.56	1016	0.63	728	0.71	1912	0.51	891	0.01	37	1.35	920	2.21	2479
	Drable	0.22	394	0.21	446	0.40	393	0.28	1107	0.33	457	0.01	32	0.99	524	0.87	976
Upstream	Covões	0.01	12	0.02	67	0.03	17	0.04	186	0.00	76	0.00	26	0.04	53	0.00	25
Sub-catchments	Esp. Santo	0.04	50	0.03	51	0.03	52	0.03	45	0.01	262	0.00	9	0.07	57	0.10	85
	Quinta	0.04	61	0.07	129	0.10	140	0.04	111	0.03	85	0.00	15	0.05	87	0.25	293

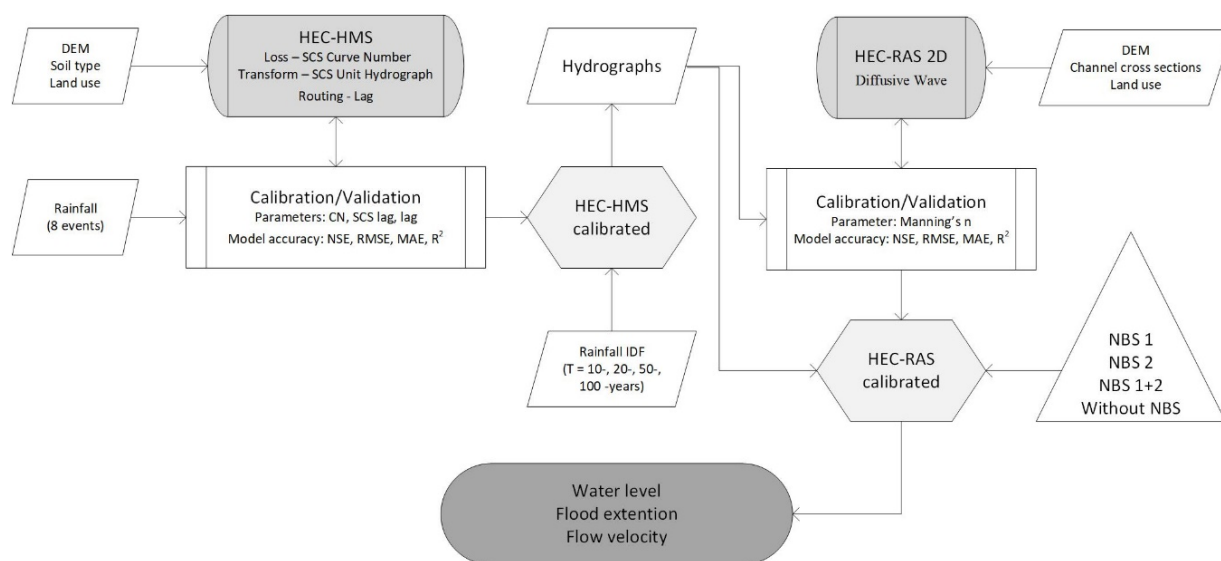


Figure 2. Flowchart of the methodology used to derive flood hazard in the Ribeira dos Covões catchment, including data inputs, main calculation methods used within the Hydrologic Engineering Center (HEC)-Hydrologic Modelling System (HMS) and hydraulic HEC-River Analysis System (RAS) models, and list of parameters used for model calibration and validation.

2.2.5. Flooding Areas with and without Nature-Based Solutions

The coupled hydrologic and hydraulic models are run, after calibration and validation, to investigate flooding caused by single events with recurrence intervals of 10, 20, 50 and 100 years. Based on rainfall derived from IDF curves of the four return period storms, HEC-HMS simulates runoff and peak discharge for the five gauging stations within Ribeira dos Covões catchment, considering a time step of 5 min. Simulated runoff and input peak flow corresponding to a given return period is converted into a stage height in HEC-RAS to simulate flood inundation area. The floodplain delineation conducted to obtain the flood inundation area involved mapping flood depth and flood extent for each of the four return periods investigated.

The HEC-RAS model is then used to assess the impact of NBS on flood inundation extent. Based on local topographical and land-use conditions, two possible sites within Ribeira dos Covões catchment which could receive and retain runoff are identified. These sites comprised abandoned fields surrounding the stream network that could be flooded without major constraints for residents and landowners. At these sites, construction of a weir at the stream margin is assumed, to divert high stream flows to the surrounding area. The weir is designed assuming an arbitrary length of 12 m and 0.75 m height, considered sufficient to deviate high streamflows to the fields that will be freely inundated. The weir is included in the HEC-RAS model by editing a depression in the DEM in ArcGIS 10.5.1. Flooding maps are prepared based on the three NBS scenarios, i.e., considering separate installation of upstream or downstream NBS (Figure 3), or a combination of both. The output flood maps of 10-, 20-, 50- and 100-year floods are analyzed and compared with the inundation maps prepared without considering the presence of NBS, in order to evaluate the potential of these flood control strategies.

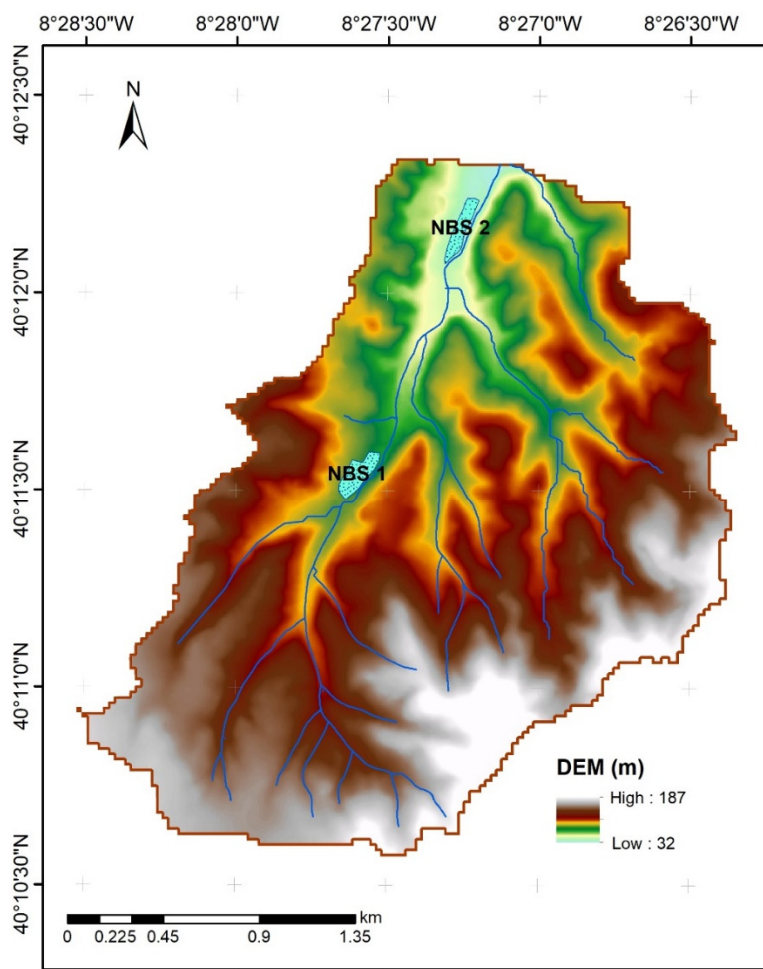


Figure 3. Location of two nature-based solutions (NBS) in the Ribeira dos Covões catchment investigated in this study, based on local settings.

3. Results

3.1. Predictive Performance of the Models

The results of the HEC-HMS model in simulating runoff from the Ribeira dos Covões catchment show good agreement with the observed streamflow in both the calibration (Table 2) and independent validation (Table 3) periods. For the catchment outlet, model accuracy during calibration (NSE = 0.91, RMSE = 0.08, MAE = 0.07, $R^2 = 0.93$) is slightly higher than in validation of runoff for the three simulated storms (NSE = 0.71–0.79, RMSE = 0.08–0.11, MAE = 0.07–0.09, $R^2 = 0.67$ –0.68). Despite the good accuracy in simulating runoff at the catchment scale, the model does not simulate accurately the runoff from the upstream sub-catchments, based on results from some evaluation criteria. For the Drable sub-catchment (Figure 1), the goodness-of-fit is highly acceptable according to all four evaluation criteria (NSE = 0.75, RMSE = 0.07, MAE = 0.05, $R^2 = 0.77$; Table 2), but the predictive performance of the model is only acceptable according to RMSE (0.01–0.10) and MAE (0.00–0.06). In the Covões sub-catchment, the model shows good goodness-of-fit and performance based only on RMSE (0.01 and 0.00–0.06, respectively) and MAE (0.01 and 0.00–0.05, respectively). However, the model for Covões still provides acceptable accuracy in the validation step for one of the storms, based on NSE (0.62) and R^2 (0.77) (Table 3). In the Espírito Santo sub-catchment, the goodness-of-fit is good for calibration and most validation periods, based on RMSE (0.02 and 0.01–0.02, respectively), MAE (0.02 and 0.01, respectively) and R^2 (0.72 and 0.57–0.73, respectively). Negative values of NSE (Tables 3 and 4) indicate that residual variance of runoff is larger than the data variance, meaning that the observed mean is a

better predictor than the model [54]. In contrast to the results for other sub-catchments, the model for Quinta shows higher accuracy in validation than calibration steps, providing acceptable performance for most storm events, including according to NSE (0.50–0.64) and R^2 (0.49–0.68).

Table 2. Goodness-of-fit of the hydrologic HEC-HMS model in simulating hourly runoff at the outlet of Ribeira dos Covões catchment (ESAC) and in four upstream sub-catchments (Drable, Covões, Quinta, Espírito Santo), based on four performance criteria (Nash–Sutcliffe efficiency (NSE), root mean square error (RMSE), mean absolute error (MAE) and coefficient of determination (R^2)). Results for the storm with best accuracy in the training step is used to parameterize and run the hydrologic model.

	ESAC	Drable	Covões	Quinta	Esp. Santo
Nash–Sutcliffe Efficiency (NSE)	0.91	0.75	−0.12	0.23	−0.31
Root Mean Square Error (RMSE)	0.08	0.07	0.01	0.03	0.02
Mean Absolute Error (MAE)	0.07	0.05	0.01	0.02	0.02
Coefficient of Determination (R^2)	0.93	0.77	0.46	0.45	0.72

Abdessamed and Abderrazak [35] report good accuracy of HEC-HMS coupled with HEC-RAS model in simulating runoff response and inundation behavior in an urban Mediterranean catchment during flood events (NSE = 0.95 during calibration). In an urban catchment in Central Texas, USA, Knebl et al. [33] report good accuracy of the HEC-HMS model (coupled with HEC-RAS) in simulating the rainfall-runoff response of 12 sub-basins during the calibration step, with MAE values ranging from 16% to 225%. Different degrees of agreement between modelled and observed discharge in different sub-catchments are more common in catchments with a greater diversity of characteristics, including soils, topography and land uses, than in more homogeneous catchments [34]. In the Ribeira dos Covões catchment, our model is less accurate in predicting discharge for the Covões sub-catchment, which comprised mixed lithology (62% limestone, 36% sandstone, and 1% alluvial deposits), than for Quinta and Espírito Santo, overlying sandstone, and Drable, located on limestone [29]. Covões also has an intermittent streamflow regime, whereas the other three sub-catchments have ephemeral streams. The model developed does not include baseflow component, and thus may underestimate water levels [34]. Annual and seasonal baseflow variations in the study area [29] are even more challenging to parameterize in intermittent streams. This may explain the greater discrepancies in predictive performance of the model when simulating discharge in different storms for Covões (e.g., NSE ranged from −0.59 and 0.62), and the differences in performance for individual events within other sub-catchments (Table 3). The general parameterization of infiltration based on soil data used in the SCS method may be inadequate to portray the heterogeneity of the Covões sub-catchment, as suggested elsewhere by Knebl et al. [33]. Use of SCS curve number to estimate infiltration and runoff at catchment and sub-catchment scales can also be a limitation in the present model, considering the different storm drainage systems. For example, although Espírito Santo has the largest proportion of urban area, occupying 49% of that sub-catchment, runoff from several sealed surfaces dissipates and infiltrates in nearby pervious areas [29], which may affect the accuracy of modelled results. According to Yuan et al. [56], CN varies with season but also with rainfall amount, with larger rainfall events showing smaller CN than smaller events. Furthermore, CN is sensitive to the fraction of initial abstraction [56].

Table 3. Predictive performance of the hydrologic HEC-HMS model in simulating hourly runoff at the outlet of Ribeira dos Covões catchment (ESAC) and in three upstream sub-catchments (Drable, Covões, Quinta, Espírito Santo) during three single validation events, based on four performance criteria (Nash–Sutcliffe efficiency (NSE), root mean square error (RMSE), mean absolute error (MAE) and coefficient of determination (R^2)).

Stream Gauge Station	ESAC			Drable			Covões			Quinta			Esp. Santo		
	1	2	3	1	2	3	1	2	3	1	2	3	1	2	3
Rainfall Event no.	1	2	3	1	2	3	1	2	3	1	2	3	1	2	3
NSE	0.73	0.79	0.17	0.31	0.50	0.64	−0.65	0.03	−0.15	−2.53	0.41	0.07	0.34	0.62	−0.59
RMSE	0.11	0.10	0.08	0.10	0.03	0.02	0.02	0.02	0.02	0.01	0.01	0.05	0.01	0.06	0.00
MAE	0.09	0.08	0.07	0.06	0.02	0.02	0.02	0.01	0.01	0.01	0.00	0.03	0.00	0.05	0.00
R2	0.82	0.82	0.67	0.48	0.64	0.68	0.49	0.57	0.73	0.26	0.43	0.24	0.35	0.77	0.34

Table 4. Goodness-of-fit (using Manning’s $n = 0.055$, which provides the best calibration results) and predictive performance of the HEC-RAS model in simulating surface water height in the stream network within the Ribeira dos Covões catchment during three separate storm events, based on four evaluation criteria (Nash–Sutcliffe efficiency (NSE), root mean square error (RMSE), mean absolute error (MAE) and coefficient of determination (R^2)).

	Calibration Event	Validation Events		
		1	2	3
NSE	0.88	0.86	0.35	−3.39
RMSE	0.06	0.03	0.09	0.07
MAE	0.05	0.02	0.07	0.07
R^2	0.95	0.88	0.80	0.34

The accuracy of the model in predicting the hydrological response of the study catchment may also have been affected by measuring errors in the gauging stations. For example, narrowing of some sections of the stream channel above Quinta, performed to facilitate movement of landowners between properties on both margins of the stream, result in overflows and runoff to surrounding areas during high rainfall events, leading to erroneous measurements at the gauging stations (Figure 4a). Land degradation enhanced by construction activities and clear-felling within the catchment may also lead to higher erosion rates and siltation [32], which may temporarily block the flow of water in some hydraulic infrastructures, consequently affecting the peak flows at downstream gauging stations (Figure 4b). Temporary siltation problems may also introduce errors in water height, especially at stream gauging stations with very low discharge, such as that in Espírito Santo (Table 1). Moreover, discharge in Quinta is affected by an upstream retention basin constructed to mitigate the impacts of business park construction, thus affecting the accuracy of peak flow in model results compared with observations.



Figure 4. Causes of erroneous measurements of high peak discharge during major storm events, leading to lower observations at upstream gauging stations than in real conditions. (a) Stream overflow due to constructed channel section constriction in Quinta sub-catchment, to allow people and animals to cross the stream; and (b) partial blockade of hydraulic infrastructure in Covões sub-catchment with sediment and litter carried during high-intensity storms.

The outputs of the calibrated and validated HEC-HMS model are used as inputs to the HEC-RAS model. The hydraulic model HEC-RAS proves useful for simulating surface water height in the Ribeira dos Covões catchment, with good accuracy in calibration (NSE = 0.83–0.88, RMSE = 0.06–0.08, MAE = 0.05–0.06, $R^2 = 0.90$ –0.95) and acceptable accuracy in validation (NSE = 0.35–0.86, RMSE = 0.03–0.09, MAE = 0.02–0.07, $R^2 = 0.80$ –0.88) for two out of three validation events (Table 4). Neither the hydrologic nor the hydraulic models perform well in validation of rainfall

event no. 3 (March 2013) characterized by the largest rainfall depth (29.2 mm), possibly due to the observation errors discussed above (Figure 4).

3.2. Flood Hazard and Impact of Nature-Based Solutions

Flood inundation results are derived for the Ribeira dos Covões catchment based on peak discharges, considering the rainfall IDF for recurrence intervals of 10-, 20-, 50- and 100-years in the meteorological model in HEC-HMS and assuming that the entire catchment received the same amount of rainfall. The peak discharge values estimated through the synthetic hydrograph method are presented in Table 5.

Table 5. Estimated peak discharge (m^3/s) at the outlet (ESAC) and at the four upstream gauging stations for 10-, 20-, 50- and 100-year floods in the Ribeira dos Covões catchment.

Gauging Stations	Recurrence Period (years)			
	10	20	50	100
ESAC	6.10	7.61	9.91	11.82
Drable	4.40	5.43	6.90	8.07
Covões	0.32	0.47	0.71	0.92
Quinta	1.02	1.31	1.79	2.23
Espírito Santo	0.35	0.41	0.51	0.60

Rainfall IDF of 10- and 100-year recurrence led to peak discharge at the catchment outlet of $6.1 \text{ m}^3/\text{s}$ and $11.8 \text{ m}^3/\text{s}$, respectively (Table 5). The Drable sub-catchment (lying on limestone), which has the largest (25% of total catchment area) and the greatest proportion of urban land use (53%) of all sub-catchments, contributed 72–68% of peak discharge at the outlet. This is driven by peak flows ranging from $4.4 \text{ m}^3/\text{s}$ to $8.1 \text{ m}^3/\text{s}$ for rainfall IDF of 10 and 100 years. The Quinta sub-catchment (lying on sandstone), occupying 24% of total catchment area but only with 25% urban land use, provides a much smaller contribution to peak discharge at the outlet (17–19%) than Drable. Espírito Santo and Covões, with similar size (11% and 10% of the catchment area) but differences in urban cover (49% and 17%, respectively) and lithology (Espírito Santo: 97% sandstone, 3% alluvium; Covões: 62% limestone, 36% sandstone, 1% alluvium), makes a minor contribution to peak discharge at the outlet (6–9% and 5–8% for 10- and 100-year floods). Although urbanization in Ribeira dos Covões has led to increased surface runoff and discharge [8,15], the location of these urban areas relative to the stream network and the type of urban pattern and storm drainage system have important impacts on runoff response [29]. In Covões, the proximity to the stream, to which urban storm runoff is piped, led to relatively high peak discharge. In contrast, the larger urban areas upslope in Espírito Santo and the dispersed drainage system (favouring runoff infiltration and retention in previous surfaces) [29] lead to relatively lower peak discharge.

Flood depth maps are prepared for return periods of 10-, 20-, 50- and 100-years, based on four simulation scenarios considering (i) current situation without NBS, and construction of a weir to deviate streamflow (ii) at an upslope location (NBS1), (iii) at a downslope location (NBS2), and (iv) at both NBS1 and NBS2 (see Figure 3). As an example, Figure 5 shows the extent of the flooded area for the four simulation scenarios with a rainfall return period of 100 years. Without NBS, the 100-year flood lead to inundation extent of 29.7 km^2 , largely located downslope near the catchment outlet. This area receives the discharge from sandstone and most of the limestone areas within Ribeira dos Covões, and lies at low altitude (Figure 3). Installation of weir sections to allow unregulated field inundation to enlarge the extent of the inundated area have a more marked effect for NBS2 than NBS1, due to the smaller magnitude of flow at the latter. Additional flooding areas of 1.2 km^2 and 9.7 km^2 are observed when implementing NBS1 or NBS2, respectively, and 2.0 km^2 when considering both NBS1 and NBS2, comparing with current conditions without NBS. In addition, it is worth mentioning that NBS2 is located in an area already prone to flooding.

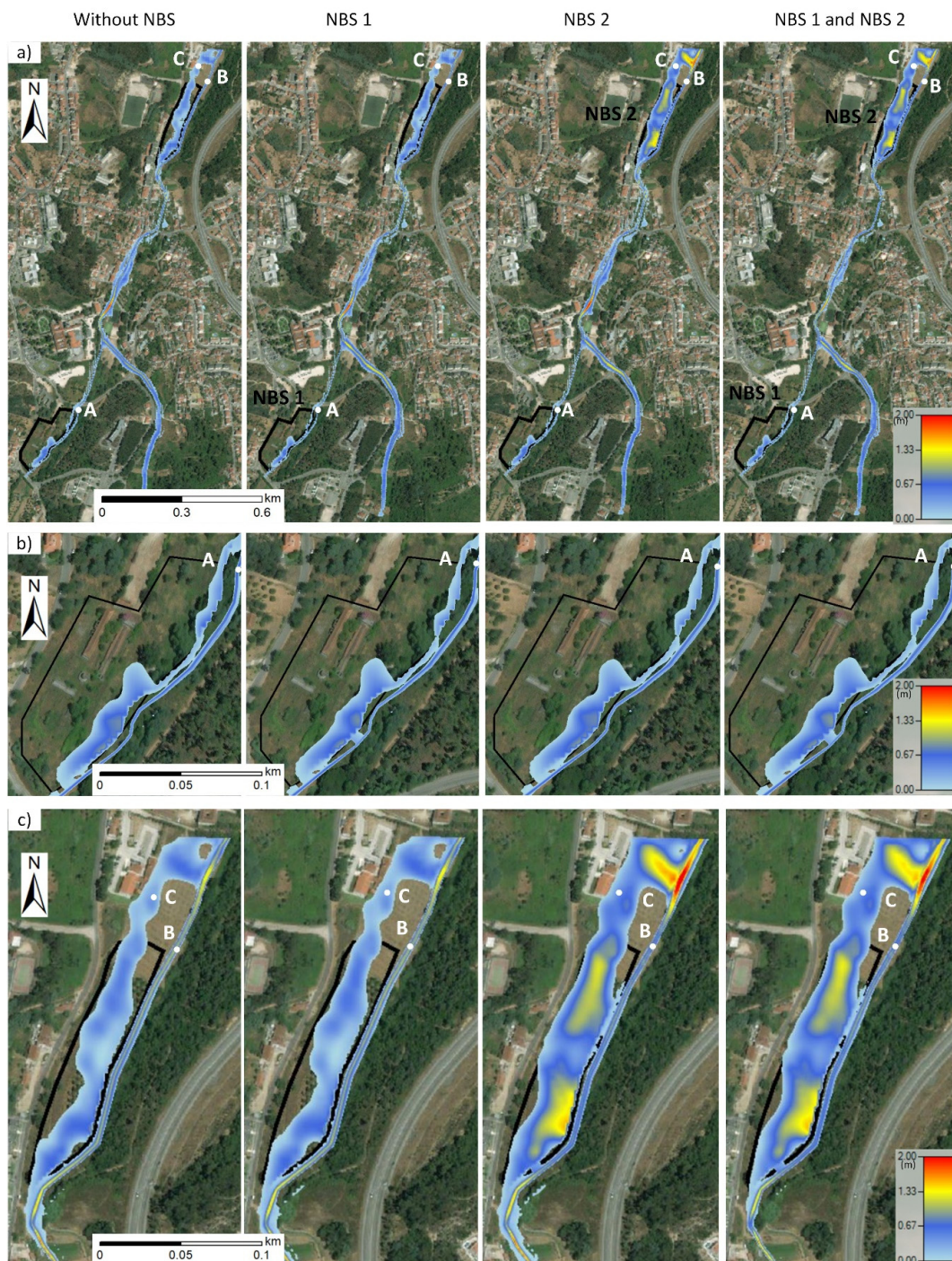


Figure 5. Flood depth maps for a return period of 100-year in four simulation scenarios (current situation without NBS, and implementation of NBS1, NBS2, and both NBS1 and NBS2), (a) showing all the drainage network within the study site, (b) with details on NBS 1 flooding area, and (c) with details on NBS2 flooding area. The letters A, B and C represent sites immediately downstream NBS1, at the catchment outlet, and on the floodplain immediately after NBS2, respectively.

Although the extent of inundated areas increases with the installation of the NBS investigated, both NBS provide lower water height within the stream network, as shown in the site examples (single grids within the inundation map) present in Figure 6. At site A (see location in Figure 5), implementation of NBS1 give a decrease of 0.06–0.07 m in water height for different return periods (Figure 5b). At the catchment outlet (site B), implementation of NBS1 lead to a 0.02 m reduction in water height for all

return periods, whereas NBS2 lead to reductions ranging from 0.10 m to 0.23 m for increasing return periods (Figure 5c). The combination of both NBS have a marginal additional impact on water height in comparison with NBS2 (additional reduction of 0.01 m for all return periods). However, at site C, located in an inundated area (Figure 5), the impact of NBS1 is apparent in a water height increase of 0.01 m and 0.02 m in 20- and 100-year floods (Figure 6). Implementation of NBS2 lead to a water height increase at the floodplain site C ranging from 0.08 m to 0.23 m, considering 10- and 100-year floods. The combination of both NBS lead to an additional increase of 0.03 m in water height comparing with NBS2. Water height in inundation areas exert a significant influence on damages [57,58].

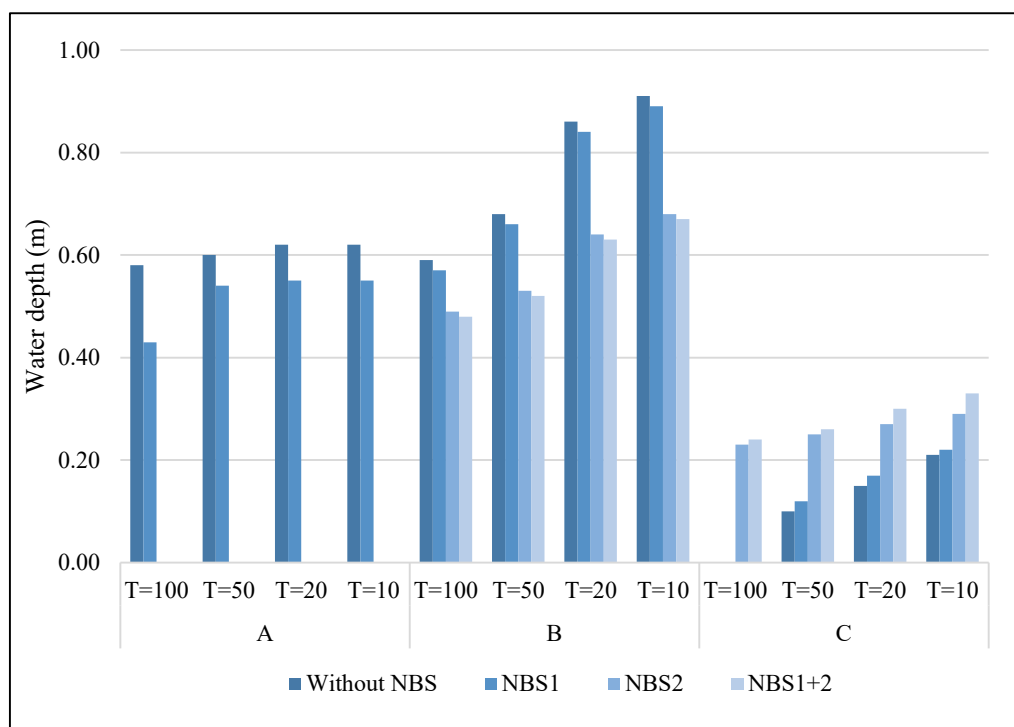


Figure 6. Mean water depth during 10-, 20-, 50- and 100-year floods for the three sites identified in Figure 5 (A, B and C) in the four simulation scenarios investigated (without NBS, and with implementation of NBS1, NBS2 and NBS1+NBS2).

NBS strategies based on the use of agriculture and rural land for flood mitigation and adaptation have been successfully used to protect downstream urban areas, which are more vulnerable and have higher economic value [59]. Flooding of specific land restores or enhances a catchment's ability to retain and slowly release stormwater using ecosystem services [60,61]. Flooding of fields can be incident-based or used only temporarily for water storage and discharge, without permanent loss of the area for human use or other ecological functions [61], as is the case for the suggested NBS in Ribeira dos Covões. Flooding of upstream fields, also called "making space for water" [62], is now a common practice, e.g., in lowland Britain, to prevent flooding of adjacent or downstream urban areas [63]. However, NBS strategies based on control flooding require more space than conventional grey infrastructures, and the land needed is often owned by private individuals [63]. Allowing specific land to flood is a particularly effective measure in flood risk control, so payments to farmers must be provided as compensation for flooding of their land [64]. Using flood-tolerant land is more cost-effective than disaster relief payments [65]. In the Stroud Frome catchment in the UK, use of floodplain areas for flood storage and additional NBS strategies to increase soil infiltration and resistance to flow by slowing the water have proven to be cost-effective [18].

In the Ribeira dos Covões catchment, the NBS scenarios investigated do not mitigate the extent of the inundated areas locally (Figure 5), since they are based on the deviation of water from stream

and allow uncontrolled inundation of the area according with terrain characteristics, i.e., elevation. However, they decrease flow rates downstream, thus making a positive contribution to reducing downslope flooding, namely outside the catchment. Long-term strategies for flood mitigation and adaptation should include various NBS, integrated into a large-scale system [63]. Small-scale NBS, which can be implemented in free spaces, are typically more efficient in reducing localized floods caused by 2-year storms [63]. NBS covering large areas (e.g., floodplains) can be more effective for large-scale flood control driven by more infrequent storms [59]. Flood risk mitigation at an extensive scale (e.g., regional) can be reduced through a network of NBS [61,65]. Good examples are the Saguenay and Red River valleys in Canada and the Engelberg Aa River in Switzerland, where a “basincentric” rather than “rivercentric” approach, which considers the whole watershed for managing flood risk, has been adopted [66].

In the study catchment, although NBS strategies are useful to mitigate flooding, few downslope urban areas require additional protection (Figure 5). Total avoidance of floods is not possible, given their climate-dependent nature and the extremely high cost of risk prevention for high-frequency events [67]. Nevertheless, a large-scale network of connected NBS strategies can help resolve urban development challenges and contribute to climate change mitigation [18]. In Ribeira dos Covões catchment, the implementation of two NBS provides higher decreases in downslope water depth (although marginal), than single NBS strategies. This may be particularly relevant in peri-urban areas, subject to high urbanization pressure, especially in the Mediterranean region, where more frequent high-intensity precipitation events are expected to increase the frequency of flood peaks [68], and where relatively limited space is available for large NBS strategies. Urbanization and climate change, coupled with hydro-meteorological risks such as floods, have a huge impact on the global economy, human well-being and the environment [69]. Thus, adequate territorial planning and NBS approaches are relevant components of sustainable solutions for flood risk reduction [70,71].

Hydrologic and hydraulic models can play an important role in supporting decision-making, since they can evaluate and predict the impact of different management strategies on current and future flood hazard, even for areas with poor data availability [5]. This is extremely useful for water management, but modelling can be challenging in heterogeneous urbanized areas, and high spatial and temporal data resolution is always desirable [5]. In the present study, coupling the HEC-HMS and HEC-RAS models proves useful for simulating the runoff response and flooding associated with current conditions and under the three NBS scenarios. However, the model developed has some limitations which may affect flood predictions. For example, the model does not include the urban storm drainage system, which can play a relevant role on hydrograph shape and response time, and thus flood velocity (reason why flood velocity results are not included in this manuscript). Including the subsurface flow and its seasonal variation in the simulation will be also relevant to improve water depth simulations [12], and thus increase the results of the evaluation criteria, particularly for the upstream sub-catchments. Furthermore, flood inundation maps prepared for current situation (without NBS) are not validated with flood observations given the lack of available data. Future work should address these limitations and focus on continuous simulations rather than single events, to better assess the flood susceptibility during wettest periods, since previous rainfall and soil moisture conditions are relevant for runoff process in Ribeira dos Covões catchment [46]. In addition, future research must focus on (i) the optimization of the NBS solutions investigated, which are currently based on the diversion of water to open fields (through a weir with arbitrary dimensions), without any consideration of flooding extent, and (ii) investigating different NBS strategies, including the connectivity of some NBS solutions, and assess their effectiveness on flood mitigation.

4. Conclusions

This paper investigates the flood hazard in Ribeira dos Covões peri-urban catchment, where floods driven by intensive rainfall events have been recorded and enhanced by urbanization. In this study, the hydrological and hydraulic response of the peri-urban catchment was successfully simulated

by coupling the HEC-HMS (NSE = 0.79, RMSE = 0.10, MAE = 0.08, $R^2 = 0.82$ in model validation), and HEC-RAS (NSE = 0.86, RMSE = 0.03, MAE = 0.02, $R^2 = 0.88$ during validation) models. The modeling approach is used to simulate surface runoff and other impacts of potential NBS measures on flood hazard mitigation, driven by storms of different return periods, by comparing the results with those from current situation without NBS. Simulation of current catchment conditions yields peak discharges at the outlet for the 10-, 20-, 50- and 100-year storms of 6.1, 7.6, 9.9 and 11.8 m³/s, respectively. These flow magnitudes lead to flood inundation in downslope catchment areas, endangering urban areas located near the stream network. The potential NBS investigated in further study simulations considers construction of a weir at various locations in the stream channel to divert high flows to abandoned surrounding fields. A simulated upslope NBS application reduces average water depth at the outlet by 0.02 m for all storm recurrence periods, which is not sufficient for mitigating floods in urban downslope areas. A simulated downslope NBS application enlarges the flooded area and reduces water depth at the catchment outlet by 0.10 m and 0.23 m for 10- and 100-year storms, respectively. The decreases in peak discharge by the downslope NBS scenario would provide considerable flood mitigation and adaptation for flood-affected areas located immediately downslope from the catchment outlet. Combination of both NBS provides marginal additional decreases in water depth at the catchment outlet of 0.09 m and 0.22 m for 10- and 100-years storms, respectively, compared with current conditions, without NBS.

The NBS approach can be useful in flood mitigation and adaptation within the study catchment, but also in downslope areas. Future studies need to further investigate the potential of other types of NBS to mitigate floods, using the combined hydrologic-hydraulic model simulation approach developed and tested in this study. Although isolated NBS measures may be primarily relevant for mitigation of local flood impacts, a strategy of network of NBS can be expected to be more effective in mitigating flood hazard over whole-catchment, and should be further investigated. The need for such large-scale NBS strategy and its implementation might be even greater for future flood mitigation, given expected increases in flood hazard driven by urbanization and climate change impacts.

Author Contributions: Conceptualization, C.S.S.F.; methodology, S.M.; formal analysis, C.S.S.F. and S.M.; writing C.S.S.F., S.M., M.K.-G., G.D. and Z.K.; funding acquisition, A.J.D.F. All authors have read and agreed to the published version of the manuscript.

Funding: This research was supported by the Portuguese Foundation for Science and Technology through (i) Post-doctoral grant SFRH/BPD/120093/201, (ii) the International Cooperation Programme for Cooperation in Science between Portugal and Serbia 2020/21 entitled “Water and sediment flows in urban and peri-urban areas”, and (iii) the Project UIDB/05183/2020. This research was also funded by Navarino Environmental Observatory (NEO) at Stockholm University.

Conflicts of Interest: The authors declare no conflict of interest.

References

1. United Nations. World Population Prospects: Highlights. 2019. Available online: https://population.un.org/wpp/Publications/Files/WPP2019_Highlights.pdf (accessed on 15 August 2020).
2. Piorr, A.; Ravetz, J.; Tosics, I. Peri-Urbanisation in Europe: Towards European Policies to Sustain Urban-Rural Futures. 2011. Available online: http://www.openspace.eca.ed.ac.uk/wp-content/uploads/2015/12/Peri_Urbanisation_in_Europe_printversion.pdf (accessed on 2 March 2018).
3. Meija, A.I.; Moglen, G.E. Spatial distribution of imperviousness and the spacetime variability of rainfall, runoff generation, and routing. *Water Resour. Res.* **2010**, *46*, W07509.
4. Jongman, B. Effective adaptation to rising flood risk. *Nat. Commun.* **2014**, *9*, 1986. [CrossRef] [PubMed]
5. Elga, S.; Jan, B.; Okke, B. Hydrological modelling of suburbanised catchments: A review and future directions. *J. Hydrol.* **2015**, *529*, 62–81.
6. Rahmati, O.; Darabi, H.; Panahi, M.; Kalantari, Z.; Naghibi, S.A.; Ferreira, C.S.S.; Kornegady, A.; Karimidastenaei, Z.; Mohamadi, F.; Stefanidis, S.; et al. Development of novel hybridized models for urban flood susceptibility mapping. *Sci. Rep.* **2020**, *10*, 12937. [CrossRef] [PubMed]

7. Loperfideo, J.V.; Noe, G.B.; Jarnagic, S.T.; Hogan, D.M. Effects of distributed and centralised stormwater best management practices and land cover on urban stream hydrology at the catchment scale. *J. Hydrol.* **2014**, *519*, 2584–2595. [[CrossRef](#)]
8. Ferreira, C.S.S.; Walsh, R.P.D.; Shakesby, R.A.; Keizer, J.J.; Soares, D.; González-Pelayo, O.; Coelho, C.O.A.; Ferreira, A.J.D. Differences in overland flow, hydrophobicity and soil moisture dynamics between Mediterranean woodland types in a peri-urban catchment in Portugal. *J. Hydrol.* **2016**, *533*, 473–485. [[CrossRef](#)]
9. Braud, I.; Breil, P.; Thollet, F.; Laagouy, M.; Branger, F.; Jacqueminet, C.; Kermadi, S.; Michel, K. Evidence of the impact of suburbanisation on the hydrological regime of a medium-sized periurban catchment in France. *J. Hydrol.* **2013**, *485*, 5–23. [[CrossRef](#)]
10. Miller, J.D.; Kim, H.; Kjeldsen, T.R.; Packman, J.; Grebby, S.; Dearden, R. Assessing the impact of suburbanisation on storm runoff in a peri-urban catchment using historical change in impervious cover. *J. Hydrol.* **2014**, *515*, 59–70. [[CrossRef](#)]
11. Leandro, J.; Schumann, A.; Pfister, A. A step towards considering the spatial heterogeneity of urban key features in urban hydrology flood modelling. *J. Hydrol.* **2016**, *535*, 356–365. [[CrossRef](#)]
12. Ferreira, C.S.S.; Walsh, R.P.D.; Steenhuis, T.S.; Ferreira, A.J.D. Effect of Peri-urban Development and Lithology on Streamflow in a Mediterranean Catchment. *Land Degrad. Dev.* **2018**, *29*, 1141–1153. [[CrossRef](#)]
13. GebreEgziabher, M.; Demissie, Y. Modeling Urban Flood Inundation and Recession Impacted by Manholes. *Water* **2020**, *12*, 1160. [[CrossRef](#)]
14. Cuny, F.C. Living with floods: Alternatives for riverine flood mitigation. *Land Use Policy* **1991**, *8*, 331–342. [[CrossRef](#)]
15. Kalantari, Z.; Ferreira, C.S.S.; Walsh, R.P.D.; Ferreira, A.J.D.; Destouni, G. Urbanization development under climate change: Hydrological responses in a peri-urban Mediterranean catchment. *Land Degrad. Dev.* **2017**, *28*, 2207–2221. [[CrossRef](#)]
16. Collentine, D.; Futter, M.N. Realising the potential of natural water retention measures in catchment flood management: Trade-offs and matching interests. *J. Flood Risk Manag.* **2016**, *11*, 76–84. [[CrossRef](#)]
17. Dong, X.; Guo, H.; Zeng, S. Enhancing future resilience in urban drainage system: Green versus grey infrastructure. *Water Res.* **2017**, *124*, 280–289. [[CrossRef](#)] [[PubMed](#)]
18. Short, C.; Clarke, L.; Carnelli, F.; Uttley, C.; Smith, B. Capturing the multiple benefits associated with nature-based solutions: Lessons from a natural flood management project in the Cotswolds, UK. *Land Degrad. Dev.* **2018**, *30*, 241–252. [[CrossRef](#)]
19. Brown, R.R.; Keath, N.; Wong, T.H. Urban water management in cities: Historical, current and future regimes. *Water Sci. Technol.* **2009**, *59*, 847–855. [[CrossRef](#)]
20. Ferreira, C.S.S.; Kalantari, Z. The Blauzone Rheintal approach from a natural hazard perspective—Challenges to establish effective flood defence management programs. In *Nature-Based Flood Risk Management in Private Land—Disciplinary Perspectives on a Multidisciplinary Challenge*; Hartmann, T., Slaviková, L., McCarthy, S., Eds.; Springer: Cham, Switzerland, 2019; pp. 161–167. ISBN 978-3-030-23841-4.
21. Sharifi, A. Urban form resilience: A meso-scale analysis. *Cities* **2019**, *93*, 238–252. [[CrossRef](#)]
22. Brillinger, M.; Dehnhardt, A.; Schwarze, R.; Albert, C. Exploring the uptake of nature-based measures in flood risk management: Evidence from German federal states. *Environ. Sci. Policy* **2020**, *110*, 14–23. [[CrossRef](#)]
23. Watkin, L.J.; Ruangpan, L.; Vojinovic, Z.; Weesakul, S.; Torres, A.S. A framework for assessing benefits of implemented nature-based solution. *Sustainability* **2019**, *11*, 6788. [[CrossRef](#)]
24. Kalantari, Z.; Ferreira, C.S.; Deal, B.; Destouni, G. Nature-based solutions for meeting environmental and socioeconomic challenges in land management and development. *Land Degrad. Dev.* **2019**, *31*, 1867–1870. [[CrossRef](#)]
25. World Bank. Implementing Nature-Based Flood Protection Principles and Implementation Guidance. 2017. Available online: <http://documents1.worldbank.org/curated/en/739421509427698706/pdf/120735-REVISED-PUBLIC-Brochure-Implementing-nature-based-flood-protection-web.pdf> (accessed on 20 April 2020).
26. Caparros-Martinez, J.L.; Milan-Garcia, J.; Rueda-Lopez, N.; de Pablo-Valenciano, J. Green infrastructure and water: And analyses of global research. *Water* **2020**, *12*, 1760. [[CrossRef](#)]
27. Nika, C.E.; Gusmaroli, L.; Ghafourian, M.; Atanasova, N.; Buttiglieri, G.; Katsou, E. Nature-based solutions as enablers of circularity in water systems: A review on assessment methodologies, tools and indicators. *Water Res.* **2020**, *183*, 115988. [[CrossRef](#)]

28. Davis, M.; Naumann, S. Making the Case for Sustainable Urban Drainage Systems as a Nature-Based Solution to Urban Flooding. In *Nature-Based Solutions to Climate Change Adaptation in Urban Areas. Theory and Practice of Urban Sustainability Transitions*; Kabisch, N., Korn, H., Stadler, J., Bonn, A., Eds.; Springer: Cham, Switzerland, 2017; pp. 123–138, 337. [[CrossRef](#)]
29. Ferreira, C.S.S.; Walsh, R.P.D.; Kalantari, Z.; Ferreira, A.J.D. Impact of Land-Use Changes on Spatiotemporal Suspended Sediment Dynamics within a Peri-Urban Catchment. *Water* **2020**, *12*, 665. [[CrossRef](#)]
30. INMG—Instituto Nacional de Meteorologia e Geofísica. 1941–2000. *Anuário climatológico de Portugal. I Parte, Continente, Açores e Madeira—Observações de Superfície*; INMG: Lisbon, Portugal. (In Portuguese)
31. Ferreira, C.S.S.; Walsh, R.P.D.; Blake, W.H.; Kikuchi, R.; Ferreira, A.J.D. Temporal dynamics of sediment sources in an urbanizing Mediterranean catchment. *Land Degrad. Dev.* **2017**, *28*, 2354–2369. [[CrossRef](#)]
32. Peña-Angulo, D.; Nadal-Romero, E.; Gonzalez-Hidalgo, J.C.; Albaladejo, J.; Andreu, V.; Barhi, H.; Bernal, S.; Biddoccu, M.; Bienes, R.; Campo, J.; et al. Relationship of weather types on the seasonal and spatial variability of rainfall, runoff and sediment yield in the western Mediterranean basin. *Atmosphere* **2020**, *11*, 609. [[CrossRef](#)]
33. Knebl, M.R.; Yang, Z.-L.; Hutchison, K.; Maidment, D.R. Regional scale flood modeling using NEXRAD rainfall, GIS, and HEC-HMS/RAS: A case study for the San Antonio River Basin Summer 2002 storm event. *J. Environ. Manag.* **2005**, *75*, 325–336. [[CrossRef](#)]
34. Thakur, B.; Parajuli, R.; Kalra, A.; Ahmad, S.; Gupta, R. Coupling HEC-RAS and HEC-HMS in Precipitation Runoff Modelling and Evaluating Flood Plain Inundation Map. In *Proceedings of the World Environmental and Water Resources Congress 2017, Sacramento, CA, USA, 21–25 May 2017*; pp. 240–251. Available online: https://digitalscholarship.unlv.edu/fac_articles/450 (accessed on 22 September 2018).
35. Abdessamed, D.; Abderrazak, B. Coupling HEC-RAS and HEC-HMS in rainfall–runoff modeling and evaluating floodplain inundation maps in arid environments: Case study of Ain Sefra city, Ksour Mountain. SW of Algeria. *Environ. Earth Sci.* **2019**, *78*, 586. [[CrossRef](#)]
36. Du, J.; Qian, L.; Rui, H.; Zuo, T.; Zheng, D.; Xu, Y.; Xu, C.-Y. Assessing the effects of urbanization on annual runoff and flood events using an integrated hydrological modeling system for Qinhui River basin, China. *J. Hydrol.* **2012**, *464–465*, 127–139. [[CrossRef](#)]
37. Costabile, P.; Costanzo, C.; Ferraro, D.; Macchione, F.; Petaccia, G. Performances of the New HEC-RAS Version 5 for 2-D Hydrodynamic-Based Rainfall-Runoff Simulations at Basin Scale: Comparison with a State-of-the Art Model. *Water* **2020**, *12*, 2326. [[CrossRef](#)]
38. U.S. Army Corps of Engineers (USACE). HEC-HMS 4.2 Modeling Users Manual. 2000. Available online: https://www.hec.usace.army.mil/software/hec-hms/documentation/HEC-HMS_Users_Manual_4.2.pdf (accessed on 31 July 2020).
39. Oleyiblo, J.O.; Li, Z.-J. Application of HEC-HMS for flood forecasting in Misai and Wan’an catchments in China. *Water Sci. Eng.* **2010**, *3*, 14–22.
40. U.S. Army Corps of Engineers (USACE). HEC-RAS 5.0 2D Modeling Users Manual. 2016. Available online: <https://www.hec.usace.army.mil/software/hec-ras/documentation/HEC-RAS%205.0%202D%20Modeling%20Users%20Manual.pdf> (accessed on 31 July 2020).
41. Geravand, F.; Hosseini, S.M.; Ataie-Ashtiani, B. Influence of river cross-section data resolution on flood inundation modeling: Case study of Kashkan river basin in western Iran. *J. Hydrol.* **2020**, *584*, 124743. [[CrossRef](#)]
42. Afshari, S.; Tavakoly, A.A.; Rajib, M.A.; Zheng, X.; Follum, M.L.; Omranian, E.; Fekete, B.M. Comparison of new generation low-complexity flood inundation mapping tools with a hydrodynamic model. *J. Hydrol.* **2018**, *556*, 539–556. [[CrossRef](#)]
43. Ezzine, A.; Saidi, S.; Hermassi, T.; Kammessi, I.; Darragi, F.; Rajhi, H. Flood mapping using hydraulic modeling and Sentinel-1 image: Case study of Medjerda Basin, northern Tunisia. *Egypt. J. Remote Sens. Space Sci.* in press. [[CrossRef](#)]
44. Brandão, C.; Rodrigues, R.; Costa, J.P. Análise de fenómenos extremos precipitações intensas em Portugal Continental. Direcção dos Serviços de Recursos Hídricos. 2001. Available online: https://snirh.apambiente.pt/snirh/download/relatorios/relatorio_prec_intensa.pdf (accessed on 1 October 2019). (In Portuguese).
45. Ferreira, C.S.S.; Ferreira, A.J.D.; de Lima, J.L.M.P.; Nunes, J.P. Assessment of surface hydrologic properties on a small urbanized mediterranean basin: Experimental design and first results. *J. Land Manag. Food Environ.* **2011**, *62*, 59–64.

46. Ferreira, C.S.S.; Walsh, R.P.D.; Steenhuis, T.S.; Shakesby, R.A.; Nunes, J.P.N.; Coelho, C.O.A.; Ferreira, A.J.D. Spatiotemporal variability of hydrologic soil properties and the implications for overland flow and land management in a peri-urban Mediterranean catchment. *J. Hydrol.* **2015**, *525*, 249–263. [[CrossRef](#)]
47. USDA. Urban Hydrology for small watersheds. In *Technical Release 55*; United States Department of Agriculture: Washington, DC, USA, 1986. Available online: https://www.nrcs.usda.gov/Internet/FSE_DOCUMENTS/stelprdb1044171.pdf (accessed on 6 April 2020).
48. Shaw, E.M. Unit hydrograph method in UK flood studies. In *Encyclopedia of Hydrology and Lakes. Encyclopedia of Earth Science*; Springer: Dordrecht, The Netherlands, 1998.
49. Chow, V.T. *Open-Channel Hydraulics*; McGraw-Hill Inc.: New York, NY, USA, 1988.
50. Nash, J.; Sutcliffe, J.V. River flow forecasting through conceptual models, part I—A discussion of principles. *J. Hydrol.* **1970**, *10*, 282–290. [[CrossRef](#)]
51. Gabellani, D.; Silvestro, F.; Rudari, R.; Boni, G. General Calibration Methodology for Combined Horton-SCS Infiltration Scheme in Flash Flood Modeling. *Nat. Hazards Earth Syst. Sci.* **2008**, *8*, 1317–1327. [[CrossRef](#)]
52. Mediero, L.; Garrote, L.; Martín-Carrasco. Probabilistic calibration of a distributed hydrological model for flood forecasting. *Hydrol. Sci. J.* **2011**, *56*, 1129–1149. [[CrossRef](#)]
53. Krause, P.; Boyle, D.P.; Bäse, F. Comparison of different efficiency criteria for hydrological model assessment. *Adv. Geosci.* **2005**, *5*, 89–97. [[CrossRef](#)]
54. Ritter, A.; Muñoz-Carpena, R. Predictive ability of hydrological models: Objective assessment of goodness-of-fit with statistical significance. *J. Hydrol.* **2013**, *480*, 33–45. [[CrossRef](#)]
55. Jeong, J.; Kannan, N.; Arnold, J. Development and Integration of Sub-hourly Rainfall–Runoff Modeling Capability Within a Watershed Model. *Water Resour. Manag.* **2010**, *24*, 4505–4527. [[CrossRef](#)]
56. Yuan, Y.; Mitchell, J.K.; Hirschi, M.C.; Cooke, R.A.C. Modified SCS Curve Number Method for Predicting Subsurface Drainage Flow. *Trans. ASABE* **2001**, *44*, 1673–1682. [[CrossRef](#)]
57. McGrath, H.; Stefanakis, E.; Nastev, M. Sensitivity analysis of flood damage estimates: A case study in Fredericton, New Brunswick. *Int. J. Disaster Risk Red.* **2015**, *14*, 379–387. [[CrossRef](#)]
58. Garrote, J.; Alvarenga, F.M.; Díez-Herrero. Quantification of flash flood economic risk using ultra-detailed stage-damage functions and 2-D hydraulic models. *J. Hydrol.* **2016**, *541*, 611–625. [[CrossRef](#)]
59. Morris, J.; Hess, T.M.; Posthumus, H. Agriculture’s role in flood adaptation and mitigation—Policy issues and approaches. In *Sustainable Management of Water Resources in Agriculture*; OECD: Paris, France, 2010; Available online: <http://www.oecd.org/water> (accessed on 4 September 2019).
60. Li, P.; Sheng, M.; Yang, D.; Tang, L. Evaluating flood regulation ecosystem services under climate, vegetation and reservoir influences. *Ecol. Indic.* **2019**, *107*, 105642. [[CrossRef](#)]
61. Metcalfe, P.; Beven, K.; Hankin, B.; Lamb, R. A modelling framework for evaluation of the hydrological impacts of nature-based approaches to flood risk management, with application to in-channel interventions across a 29 km² scale catchment in the United Kingdom. *Hydrol. Process.* **2017**, *31*, 1734–1748. [[CrossRef](#)]
62. Klijn, F.; van Buuren, M.; van Rooij, S.A. Flood-risk Management Strategies for an Uncertain Future: Living with Rhine River Floods in The Netherlands? *AMBIO A J. Hum. Environ.* **2004**, *33*, 141–147. [[CrossRef](#)] [[PubMed](#)]
63. Defra 2005. Making Space for Water. *Taking Forward a New Government Strategy for Flood and Coastal Erosion Risk Management in England*. Available online: <https://www.scribd.com/document/88816459/2005-Making-Space-for-Water-DEFRA> (accessed on 5 October 2020).
64. Hartmann, T.; Slavikova, L.; McCarthy, S. Nature-based solutions in flood risk management. In *Nature-Based Flood Risk Management on Private Land*; Hartmann, T., Slavikova, L., McCarthy, S., Eds.; Springer: Cham, Switzerland, 2019; Chapter 1, 3–9; p. 224. Available online: <https://link.springer.com/content/pdf/10.1007/978-3-030-23842-1.pdf> (accessed on 8 July 2020).
65. Holstead, K.L.; Kenyon, W.; Rouillard, J.J.; Hopkins, J.; Galán-Díaz, C. Natural flood management from the farmer’s perspective: Criteria that affect uptake. *J. Flood Risk Manag.* **2017**, *10*, 205–218. [[CrossRef](#)]
66. IFMT, 2012. Integrated Flood Management Tool Series No. 13. Conservation and restoration of rivers and floodplains. Issue 13. Available online: https://library.wmo.int/doc_num.php?explnum_id=7332 (accessed on 9 July 2020).
67. Opperman, J.J.; Galloway, G.E.; Fargione, J.; Mount, J.; Richter, B.D.; Secchi, S. Sustainable floodplains through large-scale reconnection to rivers. *Science* **2009**, *326*, 1487–1488. [[CrossRef](#)] [[PubMed](#)]

68. Peña-Angulo, D.; Nadal-Romero, E.; Gonzalez-Hidalgo, J.C.; Albaladejo, J.; Andreu, V.; Bagarello, V.; Barhi, H.; Batalla, R.J.; Bernal, S.; Gienes, R.; et al. Spatial variability of the relationships of runoff and sediment yield with weather types throughout the Mediterranean basin. *J. Hydrol.* **2019**, *571*, 390–405. [[CrossRef](#)]
69. Ruangpan, L.; Vojnovic, Z.; Di Sabatino, S.; Leo, L.S.; Capobiano, V.; Oen, A.M.P.; McClain, M.E.; Lopez-Gunn, E. Nature-based solutions for hydro-meteorological risk reduction: A state-of-the-art review of the research area. *Nat. Hazards Earth Syst. Sci.* **2020**, *20*, 243–270. [[CrossRef](#)]
70. Ourloglou, O.; Stefanidis, K.; Dimitrou, E. Assessing nature-based and classical engineering solutions for flood-risk reduction in urban streams. *J. Ecol. Eng.* **2020**, *21*, 46–56. [[CrossRef](#)]
71. Liqueste, C.; Udias, A.; Conte, G.; Grizzetti, B.; Masi, F. Integrated valuation of a nature-based solution for water pollution control. Highlighting hidden benefits. *Ecosyst. Serv.* **2016**, *22*, 392–401. [[CrossRef](#)]

Publisher’s Note: MDPI stays neutral with regard to jurisdictional claims in published maps and institutional affiliations.



© 2020 by the authors. Licensee MDPI, Basel, Switzerland. This article is an open access article distributed under the terms and conditions of the Creative Commons Attribution (CC BY) license (<http://creativecommons.org/licenses/by/4.0/>).